Science & Technology Development Journal, 24(2):1889-1897

Open Access Full Text Article

Research Article

P2- $a_{2/3}Mn_{2/3}M_{1/3}O_2$ (M = Fe, Co, Ni) cathode materials in localized high concentration electrolyte for the long-cycling performance of sodium-ion batteries

Le Minh Kha[1,2], Huynh Thi Kim Tuyen[1,2,*], Vo Duy Thanh[1,2], Nguyen Van Hoang[2,3], Tran Thanh Nhan[1,2], Tran Van Man[1,2,3], Le My Loan Phung[1,2,3]

Use your smartphone to scan this QR code and download this article

ABSTRACT

Introduction: Localized high concentration electrolytes (LHCE) have been intensively studied due to their unique properties, especially in suppressing the Na dendrite formation and long-term cycling. Therefore, the low electrochemical performance of the P2-type cathode can be overcome by using LHCE.

Methods: P2-type sodium layered oxides $Na_{2/3}Mn_{2/3}M_{1/3}O_2$ (M = Fe, Co, Ni) cathode materials were synthesized via a simple co-precipitation following a supported solid-state reaction. XRD and Rietveld method analyzed the phase composition and lattice parameters. SEM images observed the morphology of materials. The half-cell of three cathode were performed in LHCE consisting of 2.1 M sodium bis(fluorosulfonyl)imide (NaFSI) dissolved in 1,2-dimethoxyethane (DME) and bis(2,2,2-trifluoroethyl) ether (BTFE) (solvent molar ratio 1:2). The galvanostatic charge-discharge, striping-plating, and linear sweep voltage tests were carried out to investigate the electrochemical behaviors.

Results: As-prepared electrode materials exhibited discharge capacities of 94.5, 147.1, and 142.9 mAh/g at C/10 in the potential range of 1.5-4.2 V for $Na_{2/3}Mn_{2/3}Fe_{1/3}O_2$ (MFO), $Na_{2/3}Mn_{2/3}Co_{1/3}O_2$ (MCO) and $Na_{2/3}Mn_{2/3}Ni_{1/3}O_2$ (MNO), respectively. Interestingly, the MNO cathode material has a superior cycling performance with 86.5% capacity retention after 100 cycles than MCO and MFO.

Conclusion: Such superior electrochemical performance of synthesized MNO could be ascribed to the combined synergistic effects between the nickel partially substituted MNO cathode structure and using LHCE 2.1 M NaFSI/DME-BTFE (1:2). Nickel substituted MNO cathode exhibited the enhancement of discharge capacity and the long cycling stability in LHCE due to the mitigation of dendrite formation on sodium metal anode.

Key words: Sodium-ion batteries, localized high-concentrated electrolyte, P2-type sodium layered transition oxides, transition metal substitution

[1]*Department of Physical Chemistry, Faculty of Chemistry, University of Science, Ho Chi Minh city, Vietnam*

[2]*Viet Nam National University Ho Chi Minh City (VNU HCM), Ho Chi Minh city, Viet Nam*

[3]*Applied Physical Chemistry, Faculty of Chemistry, University of Science, Ho Chi Minh City, Viet Nam*

Correspondence

Huynh Thi Kim Tuyen, Department of Physical Chemistry, Faculty of Chemistry, University of Science, Ho Chi Minh city, Vietnam

Viet Nam National University Ho Chi Minh City (VNU HCM), Ho Chi Minh city, Viet Nam

Email: htktuyen@hcmus.edu.vn

History

- Received: 2020-12-30
- Accepted: 2021-05-05
- Published: 2021-05-12

DOI : 10.32508/stdj.v24i2.2508

Check for updates

Copyright

© VNU-HCM Press. This is an open-access article distributed under the terms of the Creative Commons Attribution 4.0 International license.

VNU-HCM Press

INTRODUCTION

Since its commercialization by Sony in 1991, the rechargeable lithium-ion batteries (LIBs) have been considered powerful energy storage systems for many portable electronic devices such as mobile phones, laptops, electric vehicles, etc. However, with the rapidly increasing demand for LIBs, the shortage and cost of lithium resources has driven the research community to search for new sustainable energy storage systems. Beyond Li-ion technology, sodium-ion batteries (SIBs) have been attracted as a promising alternative due to the natural abundance, worldwide distribution, and potentially low cost compared to the LIBs. Although the SIBs exhibit analog chemistry like LIBs, the development of novel cathode materials for improving energy storage performances is highly required due to the larger radius of sodium ion (0.98 Å) than lithium-ion (0.69 Å) and higher standard electrode potential of Na^+/Na (-2.71 V) compared to Li^+/Li (-3.05 V) redox couple [1–3]. Recently, layered transition metal oxide Na_xMO_2 (M = transition metals) materials have been intensively investigated due to their high volumetric energy capacity and rate capabilities, appropriate for grid application [1,4].

Sodium-based layered oxide cathode materials have been mainly categorized into two groups of O3-type and P2-type since the 1980s by C. Delmas et al. [5]. O3-type structure means that sodium ions are located in the octahedral sites with three stacking repeat MO_2 sheets of ABCABC. In P2- type structure, sodium ions occupy the prismatic sites provided by two MO_2 layers of ABBA. Notably, the P2-type layered oxide cathode materials provide a stable structure and high dif-

Cite this article : Kha L M, Tuyen H T K, Thanh V D, Hoang N V, Nhan T T, Man T V, Phung L M L. **P2-$a_{2/3}Mn_{2/3}M_{1/3}O_2$ (M = Fe, Co, Ni) cathode materials in localized high concentration electrolyte for the long-cycling performance of sodium-ion batteries**. *Sci. Tech. Dev. J.;* 24(2):1889-1897.

fusion coefficient. Hence, P2-type structure cathodes exhibit much better cycle stability and rate performance compared to the O3-type structure[6]. Among various P2-type layered transition metal oxide materials, Mn-based cathode materials (Na_xMnO_2) have been considered as the most promising candidates due to the earth-abundance, low cost, and low-toxic transition metal. Even so, P2-$Na_{0.67}MnO_2$ materials still suffer poor cycling durability owing to the strong Jahn-Teller effect associated with Mn^{3+}/Mn^{4+} redox couple and the dissolution of manganese in organic carbonated-based electrolytes[7,8]. To overcome these challenges, the partial substitution of manganese by various transition metals (e.g. Fe, Co, Ni, Cu, Mg, and Zn) in P2/P2'-$Na_{0.67}MnO_2$ structure and using advanced electrolytes instead of the conventional carbonate-based ones have been considered as promising strategies for increasing electrochemical capacity and cycling durability of the SIBs. Recently, localized high concentrated electrolytes (LHCE) have been intensively studied due to their unique properties[3,9,10]: preventing the Al current collector corrosion, wide electrochemical window, fast-chargeable ability, suppressing the Li dendrite formation, unique solvation structures, and functionalities for both LIBs and SIBs. In the previous report[3], J. Zheng and co-workers found that the LHCE containing 2.1 M NaFSI/DME-BTFE (1:2) prevents Na dendrite with high Coulombic efficiency (CE) of >99%. Moreover, this electrolyte stabilized the cycle life (upon 90.8% after 40 000 cycles) when cycling at a high current (20C) in NVP half-cell.

Herein, P2-$Na_{2/3}Mn_{2/3}M_{1/3}O_2$ cathode materials (M = Fe, Co, Ni) were prepared by a simple co-precipitation following by an assisted solid-state step. The long cycling performance of as-prepared $Na_{2/3}Mn_{2/3}Fe_{1/3}O_2$ (MFO), $Na_{2/3}Mn_{2/3}Co_{1/3}O_2$ (MCO), and $Na_{2/3}Mn_{2/3}Ni_{1/3}O_2$ (MNO) cathode materials were evaluated in a localized high concentrated electrolyte consisting of 2.1 M NaFSI/DME-BTFE (1:2) as the electrolyte compared to the conventional electrolyte based on $NaClO_4$.

MATERIALS-METHODS

Chemicals

Manganese (II) acetate tetrahydrate ($Mn(CH_3COO)_2.4H_2O$, 99%), Iron (II) sulfate heptahydrate ($FeSO_4.7H_2O$, 99.5%), Cobalt (II) nitrate hexahydrate ($Co(NO_3)_2.6H_2O$, 99%), Nickel (II) nitrate hexahydrate ($Ni(NO_3)_2.6H_2O$, 99%), 1,2-dimethoxyethane (DME, 99%), N-methyl-2-pyrrolidone (NMP, 99%) and Ethylene carbonate (EC, 99%) were purchased from Acros Organics. Sodium hydroxide (NaOH, 99%) was bought from Merck. Sodium bis(fluorosulfonyl)imide (NaFSI, 99%), Poly(vinylidene fluoride-co-hexafluoropropylene) (PVDF-HPF, M_w ~ 400,000), Poly(vinylene fluoride) (PVDF, M_w ~ 534,000), Fluoroethylene carbonate (FEC, 99%), Propylene carbonate (PC, 99.7%), Bis(2,2,2-trifluoroethyl) ether (BTFE, 98%) and Dimethyl carbonate (DMC, 99%) were purchased from Sigma-Aldrich. Deionized water (k < 2 $mS.cm^{-1}$) was used in all experiments.

Preparation of hydroxide precursors

Typically, a certain amount of $Mn(CH_3COO)_2.4H_2O$ and $FeSO_4.7H_2O$ ($Co(NO_3)_2.6H_2O$ or $Ni(NO_3)_2.6H_2O$) with a mole ratio of 2:1 were completely dissolved in 10 mL deionized water (solution A), and 25 mL of 4 M NaOH was separately prepared in a three necks glass reactor (solution B) which was connected with N_2 gas line. The metal salts mixture was precipitated by dropwise adding solution A to solution B under vigorous stirring at 50 ^oC in N_2 atmosphere for 15 h. The mixed hydroxide was filtered, rinsed with distilled water several times until the neutral solution (pH ~ 7), and the obtained sample was dried in a vacuum oven at 80 ^oC for 10 h.

P2-$Na_{2/3}Mn_{2/3}M_{1/3}O_2$ synthesis

Dried hydroxide precursors were mixed with Na_2CO_3 with a molar ratio of Na/Mn/M = 2/2/1 (M = Fe, Co, and Ni). The resultant powder was pre-calcined at 500 ^oC for 6 h in air. After cooling to room temperature, the powder was ground again. Finally, it was calcined at 900 ^oC for 36 h and then at 750 ^oC for 6 h and quenched to room temperature in Ar atmosphere. The sample was kept in an argon-filled glove box to avoid moisture from the air.

Material characterization

X-ray diffraction (XRD) patterns of as-synthesized samples were recorded at room temperature by Bruker diffractometer with Cu-Kα radiation (λ = 1.5814 Å) at the scan rate of 0.02°/step/0.25s. The phase component and crystalline structure were analyzed by using X'pert Highscore Plus software. The refinement of the lattice parameters was carried out by the Rietveld method. The morphology of these samples was observed by scanning electron microscope (SEM, Hitachi S-4800) with an accelerating voltage of 5 kV.

Preparation of localized high-concentration electrolyte

LHCE electrolyte was prepared by using a previously reported method of J. Zheng et al[3]. Typically, a volume ratio (1:2, v/v) of DME and BTFE solvents was initially until a homogenous solution. Then, a precise amount of NaFSI was weighed and slowly added to this mixture of DME and BTFE (1:2, v/v) to obtain 2.1 M salt concentration. The conventional electrolytes consisting of 1 M $NaClO_4$ dissolved in PC + 2% FEC (in vol.) and 1 M of NaFSI dissolved in EC-DMC (1:1, v/v) were also prepared for comparison. All the preparation steps were performed in the glovebox.

Coin cell assembly and electrochemical testing

The electrode composite consisting of as-prepared material, conductive carbon C65, and a binder solution PVDF-HPF (10% wt. in NMP) was mixed in a mass ratio of 80:15:5 (wt/wt/wt), respectively. This combination was thoroughly mixed in 45 minutes by using MSK-SFM-3 desk-top high-speed vibrating ball mill (MTI, USA) to obtain a homogeneous slurry. Then, the slurry was cast on aluminum (Al) current collectors by using the MSK-AFA-III automatic thick film coater (MTI, USA) and dried at 110 ^oC in a vacuum oven for 15 hours. The coated Al film was punched into 12 mm ground plates with mass loading around 2 mg/cm^2, which is matched with the dimensions of a CR2032 coin cell kit (MTI, USA). The coin cell configuration using cathode disc, sodium plate as negative, and a reference electrode, two glass fiber separators wetted by an electrolyte of 2.1 M NaFSI in DME and BTFE (1:2, v/v) (LHCE) were assembled in the glovebox. A similar procedure was carried out for two compared electrolytes. Galvanostatic discharge/charge was performed on the battery testing system (LAND, CT-2001A) in a voltage range of 1.5-4.2 V versus Na/Na^+ at currents of C/10 in the first 10 cycles and C/5 in subsequence cycles.

Long cycling performance of the Na plating/stripping processes in Na||Cu cell, in which a piece of sodium metal or Cu foil were used as an anode and a cathode separated by using a Whatman separator. The sodium plating was capacity-controlled by setting deposition time for 1 hour for currents densities of 0.5 mA/cm^2 while the stripping process was voltage controlled by setting the upper cutoff voltage to 1.0 V vs. Na^+/Na. All the cells were cycled at 25 ^oC on the LAND battery testing system.

Linear sweep voltage (LSV) measurements were carried out in Al||Na cell, in which a piece of sodium metal or Al foil were used as an anode and a cathode separated by using a Whatman separator to evaluate the oxidation stability of two different electrolytes (LCHE and conventional electrolyte) upon charging process at high potential.

RESULTS

Material characterization

X-ray diffraction (XRD) was performed to investigate the crystal structure of as-prepared sodium layered transition metal oxide materials. Figure 1 shows the Rietveld refinement of XRD patterns of MFO, MCO, and MNO samples with a low value of χ^2 factor, indicating that all patterns are well fitted with calculated models. All diffraction peaks are sharp and well-defined, which are matched well with a reference pattern of P2-$Na_{2/3}Mn_{2/3}Ni_{1/3}O_2$ (No. 00-054-0894), suggesting that all as-prepared samples reveal P2-type structure with a hexagonal $P6_3/mmc$ space group. The refined crystallographic parameters are shown in Table 1. It is observed that the crystallographic parameters of MNO and MFO are calculated to be a = b = 2.8875 Å and a = b = 2.9245 Å, respectively, which are higher than those of the MCO sample (a = b = 2.8700 Å). Such an increase of lattice parameters could be ascribed to the larger radius of Ni^{3+} (0.56 Å) and Fe^{3+} (0.55 Å) compared to that of Co^{3+} (0.545 Å)[11].

The morphologies and size of as-prepared materials were investigated by scanning electron microscopy (SEM). As shown in Figure 2, the SEM images of the MNO, MCO, and MFO exhibit some erythrocyte-like morphologies with a particle size of 0.5-1.0 μm. These particles sizes are consistent with several related sodium layered transition metal oxide cathode materials in the literature[8,12].

Electrochemical performances

The sodium cycling behavior was performed with fixed area capacity (0.5 mAh/cm^2) in Na||Cu cells using LHCE of 2.1 M NaFSI/DME-BTFE (1:2) compared to conventional carbonate-based electrolytes. Na-metal was repeatedly electroplated and stripped at a current density of 0.5 mA/cm^2 using the bare copper (Cu) foil as a substrate in these electrolytes. The estimated Coulombic efficiency (CE) for each cycle, which is measured of the reversibility and roughly calculated based on the ratio given by the capacity of Na stripped to that of Na deposited, and its CE is illustrated in Figure 3. The Na||Cu cell using LHCE reveals a negligible voltage gap between Na deposition and stripping (Figure 3a) while the one in two compared

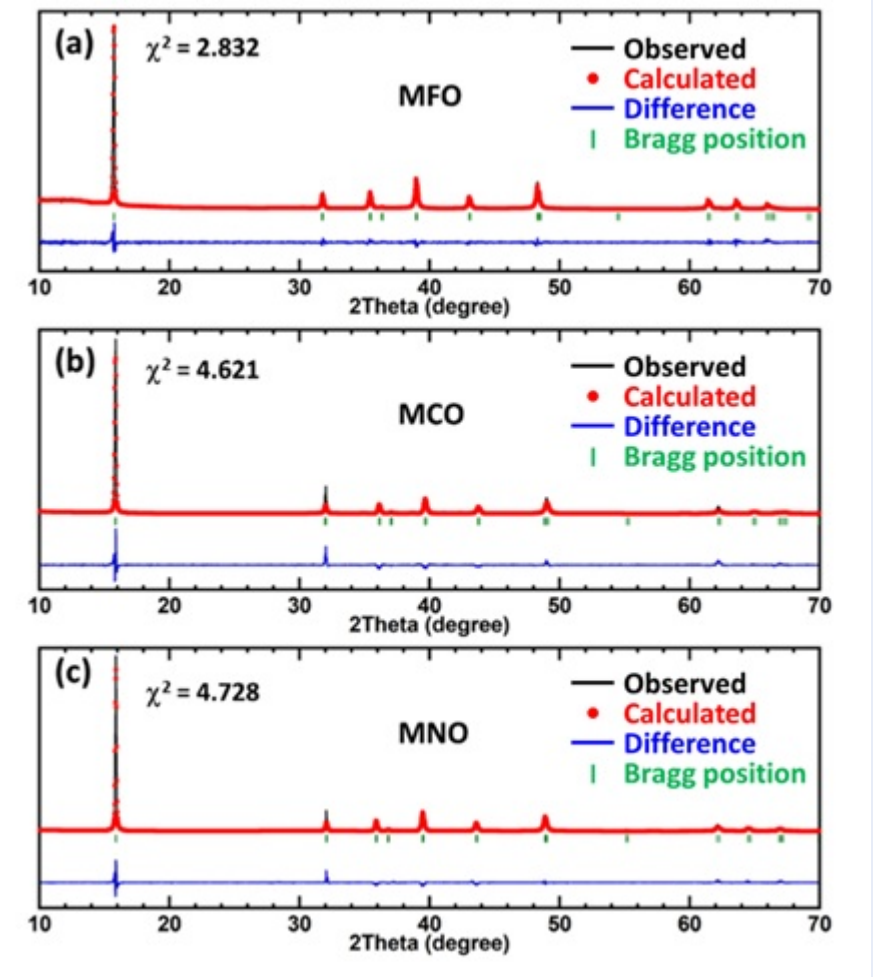

Figure 1: XRD patterns of as-prepared (a) MFO, (b) MCO and (c) MNO samples and their Rietveld refinement results

Table 1: Lattice parameters of MFO, MCO and MNO after Rietveld refinement

MFO: a = b = 2.9245 Å, c = 11.2649 Å, and V = 83.437 Å^3 MCO: a = b = 2.8700 Å, c = 11.1841 Å, and V = 79.780 Å^3 MNO: a = b = 2.8875 Å, c = 11.1606 Å and V = 80.586 Å^3				
Atoms	x	y	Z	Occupancy
Me	0	0	0	1/3
Mn	0	0	0	2/3
O	1/3	2/3	0.09	2
Na(f)	0	0	0.25	0.26
Na(e)	1/3	2/3	0.75	0.43

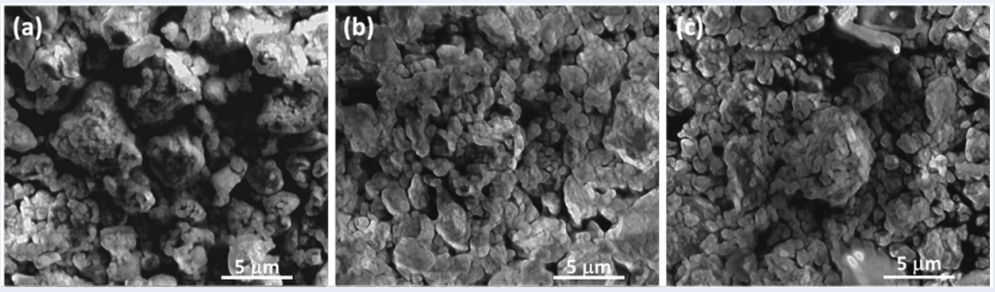

Figure 2: SEM images of (a) MFO, (b) MCO, and (c) MNO at the magnification 6500 times (scale bar 5 μm)

carbonate-based electrolytes exhibited larger voltage gaps (Figure 3b, c). Moreover, it can be observed that the Na metal CE at the first cycle is 71% in LCHE; then it is remarkably increased over 98% and maintained stable for over 100 cycles. In comparison, other electrolytes salt-solvent combinations were unable to achieve such high reversibility; typically, 1M NaFSI in carbonate solvents EC-DMC (1:1 in v/v) and 1M $NaClO_4$ in PC (2% FEC in vol. as an additive) showed very low CE, less than 30% (Figure 3d).

The galvanostatic charge-discharge tests of MFO, MCO, and MNO in LHCE were performed at 0.1 C rate in the potential window of 1.5-4.2 V. Figure 4a shows voltage profiles of the first cycle for as-prepared MFO, MCO, and MNO cathode materials, in which charging curves reveal a distinctive slope and a plateau region corresponding to redox couples of Mn^{3+}/Mn^{4+} and M^{3+}/M^{4+}. It is noticeable that MFO and MCO charging curves exhibit a higher slope compared to the potential curve of MNO, indicating the higher activated Mn^{3+}/Mn^{4+} content for MNO. Besides, MCO and MNO showed a large difference in discharge capacities between charge and discharge processes, whereas the ratio of capacities between charge and discharge processes for the case of MFO exhibits nearly a unit. This may be due to higher porosity in the P2 structure of MCO and MNO compared to that of MFO, resulting in the improvement of Na^+ diffusion in the initial host structure. As shown in Figure 4b-d, the capacity differences for MFO between the 5^{th}, 10^{th} cycle (with a rate of 0.1 C) and 20^{th}, 50^{th} cycle (with a rate of 0.2 C) seem to be larger than those of MCO and MNO cathode materials. The poor cycling performance of MFO can be originated from both Jahn–Teller distortion and the unstable structure when oxidation potential raising over 4.0 V, at which the Fe^{3+} species can be converted to $Fe^{4+,}$ leading to structural instability and capacities fading. Moreover, in carbonate-based solvents, NaFSI is oxidized at the potential of over 3.95 V. However, the oxidation potential is much higher for the commonly used electrolyte of 1 M $NaClO_4$/PC + 2% FEC (in vol.), as shown in the LSV result (Figure 5). Therefore, this electrolyte is not compatible with P2-$Na_{2/3}Mn_{2/3}M_{1/3}O_2$ cathode due to its high upper cutoff voltage (4.2 V). The poor charge/discharge curves of MNO and MFO in the electrolyte 1 M NaFSI/EC-DMC (1:1) have been strongly related to this phenomenon.

These results are correlated to the NaFSI salt in carbonate-based solvents, which is the factor leading to Al corrosion[13]. Meanwhile, P2-$Na_{2/3}Mn_{2/3}M_{1/3}O_2$ exhibited good properties when cycling in LHCE electrolyte due to its oxidation stability at the working voltage of the cathode. As a result, LHCE has successfully prevented the Al current collector from corroding with FSI^- anion.

The cycling performances of all as-prepared cathode materials are shown in Figure 6. Notably, the first 10 cycles were measured at 0.1 C, while a current density of 0.2 C was applied for the cycles from the 11^{th}-100^{th} cycle. The discharge capacities of MFO, MCO, and MNO are obtained from the 2^{nd} cycle, which is 94.5, 147.1, and 142.9 mAh/g, respectively. After 10 cycles, the MFO, MCO, and MNO exhibit capacities retention of 92.2, 97.0, and nearly 100% at the rate of 0.1 C, respectively. A similar trend of capacities retention for the cycles from the 11^{th}-100^{th} at 0.2 C, whereas the MNO reveals remarkable cycling performance of 86.5% compared to that of MCO (81.8%) and MFO (65.8%). Moreover, CE of all as-synthesized samples reaches nearly 98% except for the initial CE (1^{st} cycle), indicating the high reversibility of deintercalation/intercalation reactions of Na^+ ions with the cathode materials in the LHCE system.

DISCUSSION

As mention in the results section, the electrolyte LHCE consists of 2.1 M NaFSI dissolved in DME

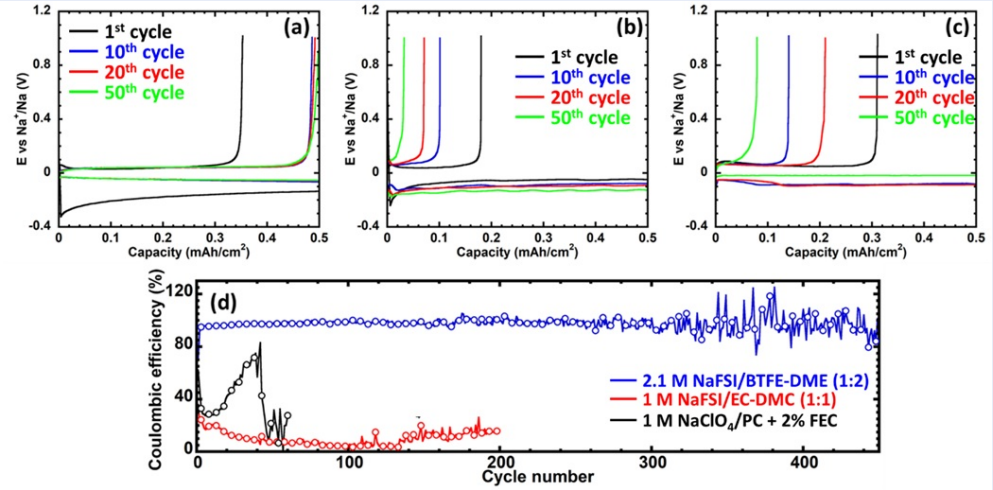

Figure 3: Voltage profile of Na plating-stripping processes in (a) 2.1 M NaFSI/BTFE-DME (1:2), (b) 1 M NaFSI/EC-DMC (1:1), (c) 1 M $NaClO_4$/PC + 2% FEC and their Coulombic efficiency with cycling measured in Na||Cu cell (d) by repeated plating and stripping processes at 0.5 mA/cm^2

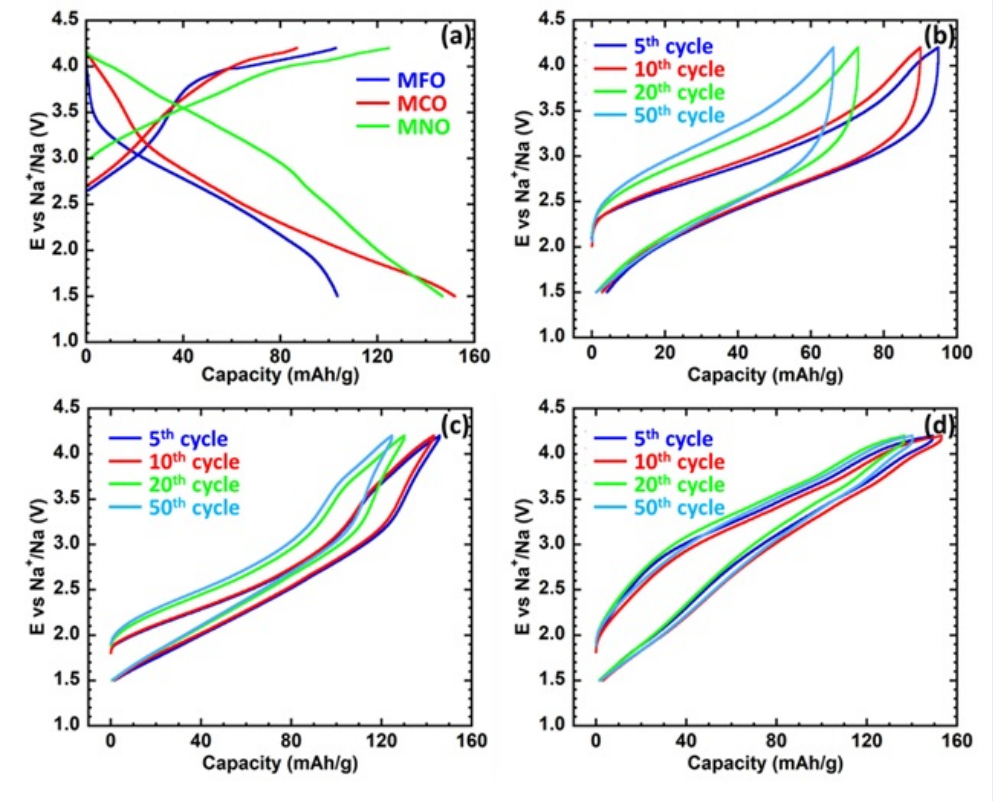

Figure 4: (a) Charge and discharge profiles of MFO, MCO, and MNO at 0.1 C for the first cycle. The voltage profiles of different cycles at 0.2 C for (b) MFO, (c) MCO, and (d) MNO

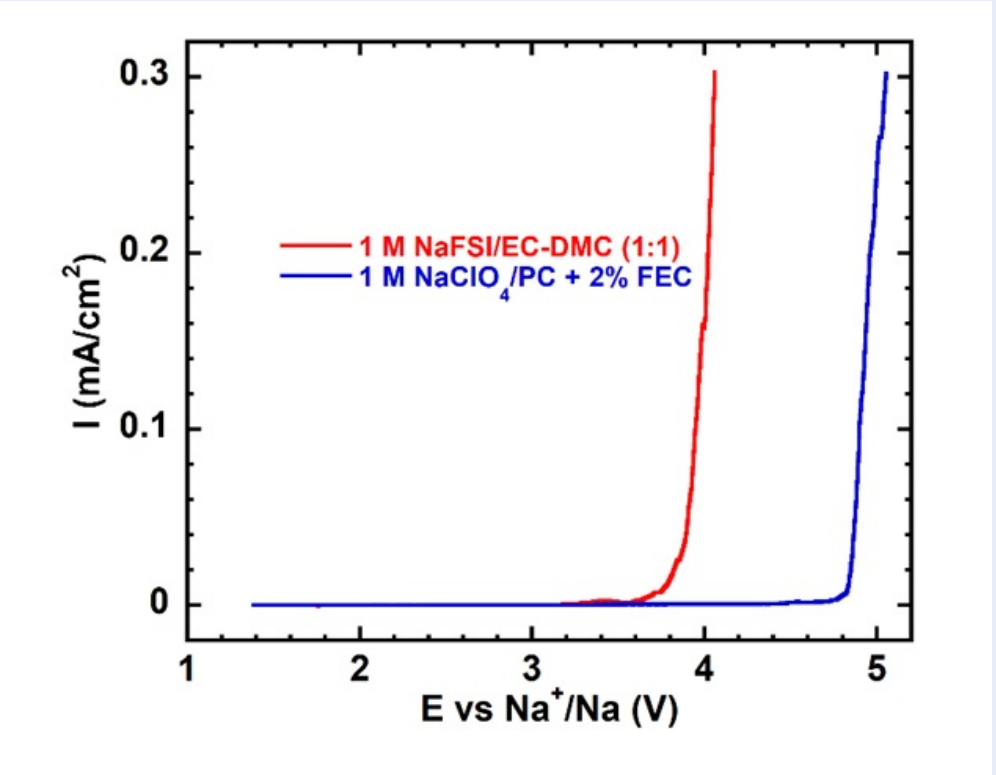

Figure 5: Oxidation ability of some carbonate-based electrolytes: 1 M NaFSI/EC-DMC (1:1) (red line) and 1 M NaClO4/PC + 2% FEC (blue line)

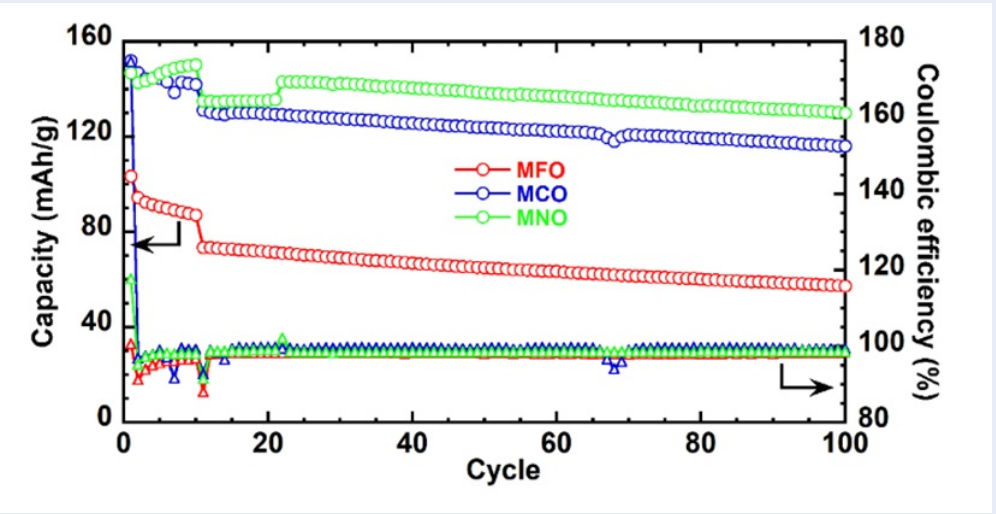

Figure 6: Cycling performances of MFO, MCO, and MNO at 0.1 C in the first 10 cycles and at 0.2 C after 10 cycles and their corresponding Coulombic efficiencies

and BTFE (1:2, v/v) can overcome the disadvantages of low concentration carbonate-based solvents. LHCE can prevent the corrosion of Al current collector caused by FSI- anion. It can be explained by the solvation of ions becoming more strongly in LHCE, which obstructs the reaction between FSI- anion and Al at a low voltage of 3.7 V (Figure 5). Additionally, using LHCE pushes the efficiency of sodium plating/striping up to nearly 100%. In the stripping-plating technique (Figure 3), Na can be electrostripping and electroplating almost reversibly, indicating that LHCE can be used as a promising electrolyte for anode-free cells.

The high content of sodium salts in the composition of LHCE leads to the high cost of the electrolyte and also increases the viscosity that lowers the ionic conductivity. Therefore, the capacity of MFO, MNO, and MCO materials cycling in LHCE are lowered than other carbonate-based electrolytes[8,14]. The capacity is contributed by the oxidation/reduction couples of the doped element M^{4+}/M^{3+} and Mn^{4+}/Mn^{3+} increases in order: MNO > MCO > MFO. The high agglomeration, the bigger the particle size of MFO that hinders the kinetics, can contribute to the low capacity. On the other hand, Ni is active species and possesses 2 electrons mechanism that brings additional capacity to MNO material[15]. Interestingly, it is noticeable that LHCE can enable the long-term cycling of these materials, which was an important factor for grid-scale energy storage systems.

CONCLUSION

The effects of transition metal (Fe, Co, Ni) substitution in the structure of P2-$Na_{2/3}Mn_{2/3}M_{1/3}O_2$ and their electrochemical behaviors with the localized high concentrated electrolyte of 2.1 M NaFSI/DME-BTFE (1:2) have been successfully investigated. It was found that the MNO shows a high specific capacity of 142.9 mAh/g and outstanding cycling performance with 86.5% capacities retention after 100 cycles at 0.2 C compared to the MCO and MFO. Such remarkable electrochemical performance at MNO could be attributed to the Ni doping in the cathode structure, helping to mitigate the Jahn-Teller effect and stabilize layered oxide structure. Also, the LHCE system plays a vital role in preventing dendrite formation at the sodium anode, thus enhances long-term cycling durability and suppress the Al corrosion causing by FSI^- anion, which are critical points for the practical application of sodium-ion batteries.

ACKNOWLEDGMENTS

This research is funded by Viet Nam National University of Ho Chi Minh City (VNU-HCM) under grant code C2020-18-24.

COMPETING INTERESTS

The authors declare that there is no conflict of interest.

AUTHOR'S CONTRIBUTIONS

Le Minh Kha synthesized the materials, characterized the materials, and wrote the paper; Huynh Thi Kim Tuyen optimized the design idea; Nguyen Van Hoang and Tran Thanh Nhan edited the craft; Vo Duy Thanh investigated the electrochemical behaviors of materials in LHCE; Tran Van Man performed the analysis, and Le My Loan Phung proposed the research idea.

ABBREVIATION

LIB: lithium-ion battery
SIB: Sodium-ion battery
MFO: $Na_{2/3}Mn_{2/3}Fe_{1/3}O_2$
MCO: $Na_{2/3}Mn_{2/3}Co_{1/3}O_2$
MNO: $Na_{2/3}Mn_{2/3}Ni_{1/3}O_2$
LHCE: localized high concentrated electrolyte
CE: Coulombic efficiency

REFERENCES

1. Clément RJ, Bruce PG, Grey CP. Manganese-based P2-type transition metal oxides as sodium-ion battery cathode materials. Electrochem. Soc. 2015;162(14):A2589-A604;Available from: https://doi.org/10.1149/2.0201514jes.
2. Li F, Wei Z, Manthiram A, Feng Y, Ma J, Mai L. sodium-based batteries: from critical materials to battery systems. J. Mater. Chem. A. 2019;7(16):9406-31;Available from: https://doi.org/10.1039/C8TA11999F.
3. Zheng J, Chen S, Zhao W, Song J, Engelhard MH, Zhang J-G. Extremely stable sodium metal batteries enabled by localized high-concentration electrolytes. ACS Energy Lett. 2018;3(2):315-21;Available from: https://doi.org/10.1021/acsenergylett.7b01213.
4. Rong X, Liu J, Hu E, Liu Y, Wang Y, Wu J, Yu X, Page K, Hu Y-S, Yang W. Structure-induced reversible anionic redox activity in Na layered oxide cathode. Joule. 2018;2(1):125-40;Available from: https://doi.org/10.1016/j.joule.2017.10.008.
5. Delmas C, Fouassier C, Hagenmuller P. Structural classification and properties of the layered oxides. Physica B + C. 1980;99(1-4):81-5;Available from: https://doi.org/10.1016/0378-4363(80)90214-4.
6. Kumakura S, Tahara Y, Sato S, Kubota K, Komaba S. P'2-Na2/3Mn0.9Me0.1O2 (Me = Mg, Ti, Co, Ni, Cu, and Zn): correlation between orthorhombic distortion and electrochemical property. Chem. Mater. 2017;29(21):8958-62;Available from: https://doi.org/10.1021/acs.chemmater.7b02772.
7. Zhang J, Wang W, Wang W, Wang S, Li B. Comprehensive review of P2-Type Na2/3Ni1/3Mn2/3O2, a potential cathode for practical application of Na-Ion batteries. ACS Appl. Mater. Interfaces 2019;11(25):22051-66;PMID: 31136141. Available from: https://doi.org/10.1021/acsami.9b03937.
8. Zhang Y-Y, Zhang S-J, Li J-T, Wang K, Zhang Y-C, Liu Q, Xie R-S, Pei Y-R, Huang L, Sun S-G. Improvement of electrochemical properties of P2-type Na2/3Mn2/3Ni1/3O2 sodium ion battery cathode material by water-soluble binders. Electrochim. Acta. 2019;298:496-504;Available from: https://doi.org/10.1016/j.electacta.2018.12.089.

9. Shi PC, Lin M, Zheng H, He XD, Xue ZM, Xiang HF, Chen CH. Effect of propylene carbonate-Li+ solvation structures on graphite exfoliation and its application in Li-ion batteries. Electrochim. Acta. 2017;247:12-8;Available from: https://doi.org/10.1016/j.electacta.2017.06.174.
10. Doi T, Shimizu Y, Hashinokuchi M, Inaba M. LiBF4-Based concentrated electrolyte solutions for suppression of electrolyte decomposition and rapid lithium-ion transfer at LiNi0.5Mn1.5O4/electrolyte interface. Electrochem. Soc. 2016;163(10):A2211;Available from: https://doi.org/10.1149/2.0331610jes.
11. Shannon RD. Revised effective ionic radii and systematic studies of interatomic distances in halides and chalcogenides. Acta Crystallogr. 1976;32(5):751-67;Available from: https://doi.org/10.1107/S0567739476001551.
12. Zhao J, Xu J, Lee DH, Dimov N, Meng YS, Okada S. Electrochemical and thermal properties of P2-type Na2/3Fe1/3Mn2/3O2 for Na-ion batteries. J. Power Sources. 2014;264:235-9;Available from: https://doi.org/10.1016/j.jpowsour.2014.04.048.
13. Ponrouch A, Monti D, Boschin A, Steen B, Johansson P, Palacín MR. Non-aqueous electrolytes for sodium-ion batteries. J. Mater. Chem. A. 2015;3(1):22-42;Available from: https://doi.org/10.1039/C4TA04428B.
14. Yabuuchi N, Kajiyama M, Iwatate J, Nishikawa H, Hitomi S, Okuyama R, Usui R, Yamada Y, Komaba S. P2-type Nax[Fe1/2Mn1/2]O2 made from earth-abundant elements for rechargeable Na batteries. Nat. Mater. 2012;11(6):512-7;PMID: 22543301. Available from: https://doi.org/10.1038/nmat3309.
15. Hou P, Zhang H, Zi Z, Zhang L, Xu X. Core-shell and concentration-gradient cathodes prepared via co-precipitation reaction for advanced lithium-ion batteries. Journal of Materials Chemistry A. 2017;5(9):4254-79;Available from: https://doi.org/10.1039/C6TA10297B.